JOURNAL OF VETERINARY MEDICAL RESEARCH 2019, 26 (2): 271-279

Journal homepage:
http://www.bsu.edu.eg/bsujournals/JVMR.aspx

Online ISSN: 2357-0520 Print ISSN: 2357-0512

Original Research Article

Normal cross-sectional anatomy and magnetic resonance imaging of pastern and coffin joints in camel

Ibrahim, A.A.H.*, **Adam, Z.E. and Tawfiek, M.G.**
Anatomy and Embryology Department, Faculty of Veterinary Medicine, Beni-Suef University, Beni-Suef 62511, Egypt.

ABSTRACT

The present study aimed to describe the normal cross sectional anatomy and magnetic resonance imaging of pastern and coffin joints in dromedary camel. This study was conducted on twelve distal limbs (fore and hind) of fresh cadavers from three adult camels of both sexes. The specimens appeared normal without orthopedic disorders. Twelve distal limbs were scanned using a 1 Tesla MRI scanner and then injected with colored latex to be sectioned into sagittal, dorsal and transverse slices. Cross anatomical sections were matched with their corresponding MR images for identification and evaluation of the clinically relevant anatomical structures that appeared with different signal intensities on MRI scans. The present study showed that all major soft tissues in pastern and coffin joints of camel were clearly depicted on MR images, however, the palmar/plantar ligaments of pastern joint and ligaments of navicular cartilage could not be identified on MR images. The annotated cross anatomical sections with the corresponding MR images could be used as a normal reference for interpretation of some clinical diseases in pastern and coffin joints of camel.

ARTICLE INFO

Article history:

Received

29/4/ 2019

Accepted

30/7/2019

Online 2/8/2019

Keywords:
Camel, Coffin joint, Magnetic resonance imaging, Pastern joint

***Corresponding author: Ibrahim, A.A.H.**, Anatomy and Embryology Department, Faculty of Veterinary Medicine, Beni-Suef University, Beni-Suef 62511, Egypt.
Email: d.azzamohamed88@gmail.com

1. Introduction

Camel population is found in Egypt, Saudi Arabia, Iraq, Sudan, Iran, Somaliland, India, China and many other countries (Monfared, 2013). Camel is capable to overcome harsh climate of desert and able to survive and produce under difficult environmental conditions (Sadegh et al., 2007). In developing countries, it is used as an essential source of milk, meat and hide (Ahmad et al., 2010).

Lameness is a critical problem due to its adverse economic impact on dairy animals (Solano et al., 2015). In addition, lameness in camel appears with a different pattern compared to bovine and equine, due to particular anatomy of camel (Al-Juboori, 2013). These conditions require awareness of the normal gross anatomical structure and improvement of high definitive diagnostic imaging techniques for clarification and evaluation of the orthopedic affections.

There is a growing awareness in using magnetic resonance imaging (MRI) and computed tomography (CT) as high definitive diagnostic imaging techniques in veterinary practices (Nuss et al., 2011). However, limited accessibility, need for animal general anesthesia and high costs diminish using these techniques in veterinary medicine (Arencibia et al., 2000). Nevertheless, improvement in accessibility and availability of these modalities increases the requirement of their use in animal medicine (Pollard and Puchalski, 2011). Even though many MRI studies had been done on animal digits (El-Nahas et al., 2015 in camel; Abdellatif et al., 2018 in bovine; Sampson and Tucker, 2007 in horse), however, more details on cross sectional anatomy in matching to MRI are still needed on pastern and coffin joints of dromedary camel.

The current study aimed to provide a detailed anatomic reference on cross sectional anatomy and MRI of the pastern and coffin joints in camel to assist as a helpful database for evaluation of clinical disorders in these joints.

2. Materials and methods

2.1. Animals

The current study was carried out on twelve distal fore and hind limbs (n=12) of fresh cadavers from three dromedary camels (2-4 years old, weighed about 350-500 kg.). These limbs were obtained from the slaughterhouse at Beni-Suef Governorate, these specimens were apparently normal with no musculoskeletal disorders. MRI examination was achieved on twelve distal limbs (Forelimb; n=6, hind limb; n=6) of fresh cadavers, this examination was performed within three hours after euthanasia. Then the limbs were frozen and sectioned for preparation of transverse, dorsal and sagittal slices with 1cm thickness.

2.2. Magnetic resonance imaging

Limbs were located with their palmar/ plantar aspects as the dependent portion and their long axis perpendicular to the examination table. T1-weighted MR images (TR= 1900ms, TE=2.74ms, slice thickness= 2mm) were obtained in sagittal, dorsal and transverse planes using a 1 Tesla magnet (Philip Medical System Intera).

2.3. Preparation of the anatomical cross sections

The scanned limbs were injected with colored latex. The needle was introduced into the dorsal pouches of the pastern and coffin joints abaxial to the tendinous parts of the digital extensor tendons. Then the limbs were frozen at -20^{o}C for 7 days, and sectioned into sagittal (Forelimb; n=2, hind limb; n=2), dorsal (Forelimb; n=2, hind limb; n=2) and transverse (Forelimb; n=2, hind limb; n=2) slices starting at the middle of the first phalanx till the coffin joint in 1cm slice thickness by using an electric band saw. Tap water was used for gentle cleaning of the anatomic sections to be photographed.

The anatomical sections were grossly inspected, determined and selected in correlation to their corresponding MR images.

2.4. Comparison of cross anatomical sections with MR images

The cross sections of pastern and coffin joints were compared to their corresponding MR images. For evaluation of the anatomical structures of pastern and coffin joints, six MR images were selected in correspondence to the anatomical structures of the anatomical cross sections of the same specimens, one in a sagittal plane (Fig. 1), one in a dorsal plane (Fig. 2) and four in transverse planes (Figs. 3-6).

3. Results

The compared cross anatomical sections and magnetic resonance images (MRI) gave a reference for precise interpretation of the MRI of pastern and coffin joints in camel. Articular cartilages of second and third phalanges were clearly differentiated from the bony structures as a thin plate of high signal intensity (Figs. 1, 2). Subchondral bone was visualized as a thin layer of low signal intensity which could be easily recognized from articular cartilage at the extremity of each bone (Figs. 1, 2). Cancellous bone appeared at extremities of second and third phalanges with high signal intensity (Figs. 1, 2). The medullary cavity of second and third phalanges appeared with a high signal intensity, while cortical bone could be visualized with a low signal intensity (Figs. 1, 2). A middle scutum and navicular cartilage were clearly defined on sagittal MR images with a high signal intensity (Fig. 1). Moreover, the nails had a heterogeneous high signal intensity (Fig. 1), while the sole of the footpad appeared as a layer of low signal intensity between two lines of high signal intensity (Figs. 1, 2). Digital cushion had heterogeneous high signal intensity, and the surrounding tissue had intermediate signal intensity on sagittal and dorsal MR images (Figs. 1, 2).

Soft tissue structures were easily visualized on MRI with variable signal intensities. Extensor tendons which could be identified on MR images included; lateral digital extensor tendons, lateral and medial limbs of the common digital extensor tendons. These tendons appeared with homogenous low signal intensity. Margins of these tendons could be defined by the surrounded fascia which had low intermediate signal intensity. The extensors were best identified on transverse MR images as two small oval structures on dorsal aspect of each digit (Fig. 3). Distal to the pastern joint, these tendons were constituted by one narrow strip on the dorsal aspect of each digit representing the branches of lateral limb of common digital extensor tendon (Fig. 4, 5). Moreover, insertion of the lateral limb of the common digital extensor tendon in the dorsal ridge of the third phalanx was clearly depicted on sagittal MR images (Fig. 1).

Superficial digital flexor tendon (SDFT) and deep digital flexor tendon (DDFT) had low signal intensity surrounded by digital tendon sheaths which appeared with low signal intensity (Figs. 3-6). At the distal third of first phalanx, SDFT appeared deep to DDFT prior to its insertion on proximal extremity of the second phalanx (Fig. 3). palmar/plantar to the middle scutum, DDFT appeared as a semi-circular structure (Fig. 4), while distal to pastern joint, this tendon became flattened in shape (Fig. 5, 6). The reposition of the flexor tendons could be also visualized on sagittal MR images (Fig. 1). Moreover, the inserted part of DDFT on flexor surface of the third phalanx was separated from the underlying digital cushion by a bursa which well-defined on sagittal MR images with a low signal intensity (Fig. 1).

Joint capsules of pastern and coffin joints had low signal intensities, while their margins were outlined as thin lines of intermediate signal intensity on all MR images (Figs., 1-6). Ligaments of these joints were well-delineated on transverse and dorsal MR images with intermediate signal intensity (Figs. 1, 2). The ligaments which could be clearly outlined on MR images included; collateral ligaments of the pastern joint, as well as the interdigital, collateral and dorsal ligaments of the coffin joint. While palmar/plantar ligaments of the pastern joint and ligaments of navicular cartilage could not be defined.

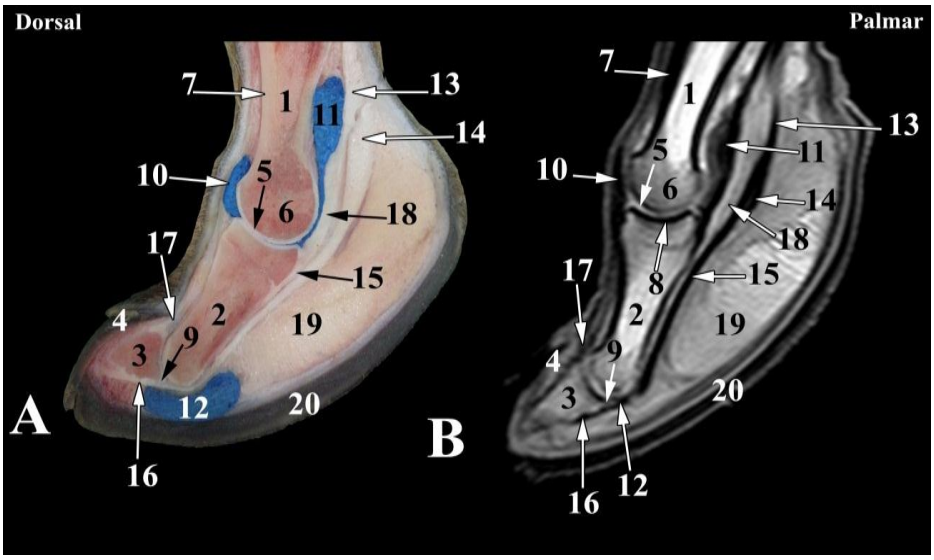

Fig. 1 Sagittal images of right fore distal limb of camel. A- Sagittal anatomical section; B- Magnetic resonance image: 1- First phalanx; 2- Second phalanx; 3- Third phalanx; 4- Nail; 5- Articular cartilage; 6- Cancellous bone; 7- Cortical bone; 8- Subchondral bone; 9- Navicular cartilage; 10- Dorsal synovial pouch of pastern joint; 11- Palmar/plantar synovial pouch of pastern joint; 12- Bursa between insertion of deep digital flexor tendon and digital cushion; 13- superficial digital flexor tendon; 14- Deep digital flexor tendon; 15- Insertion of superficial digital flexor tendon; 16- Insertion of 1deep digital flexor tendon; 17- Insertion of lateral limb of common digital extensor tendon; 18- Middle scutum; 19- Middle digital cushion; 20- Sole.

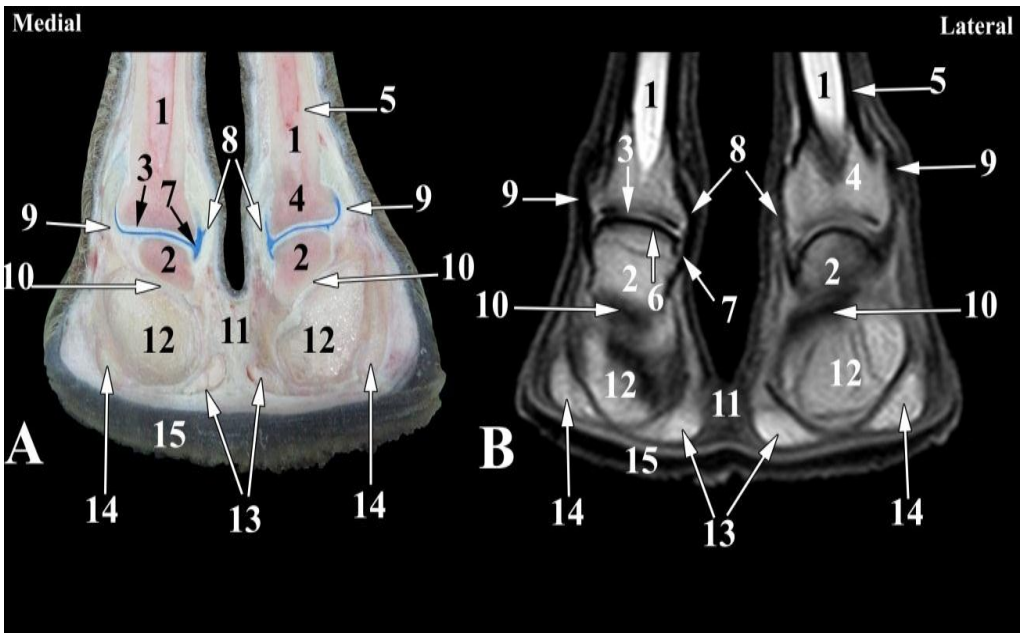

Fig. 2 Dorsal images of pastern joint right fore limb of camel at the level of collateral ligaments attachment. A- Dorsal anatomical section; B- Magnetic resonance image: 1- Proximal phalanx; 2- Middle phalanx; 3- Articular cartilage; 4- Cancellous bone; 5- Cortical bone; 6- Subchondral bone; 7- Joint cavity of pastern joint; 8- Axial collateral ligaments of pastern joint; 9- Abaxial collateral ligaments of pastern joint; 10- Deep digital flexor tendon; 11- Interdigital ligament; 12- Middle digital cushion; 13- Axial digital cushion; 14- Abaxial digital cushion; 15- Sole.

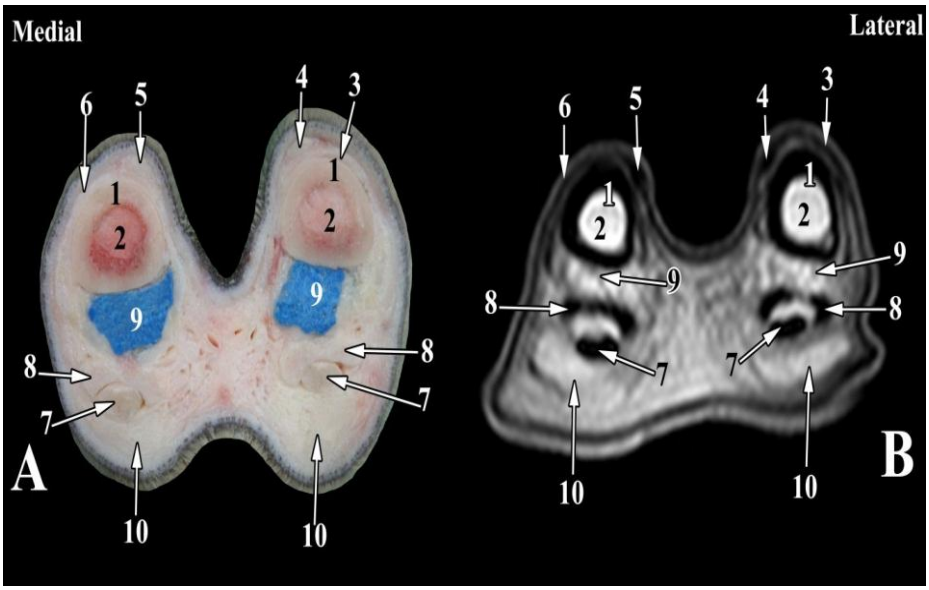

Fig. 3 Transverse images of right fore distal limb of camel at the level of distal third of proximal phalanges. A- Transverse anatomical section; B- Magnetic resonance image: 1- Proximal phalanx; 2- Medullary cavity of proximal phalanx; 3- Lateral digital extensor tendon; 4- Lateral branch of lateral limb of common digital extensor tendon; 5- Medial branch of lateral limb of common digital extensor tendon; 6- Medial limb of common digital extensor tendon; 7- Deep digital flexor tendon; 8- Superficial digital flexor tendon; 9- Palmar synovial pouch of pastern joint; 10- Digital cushion.

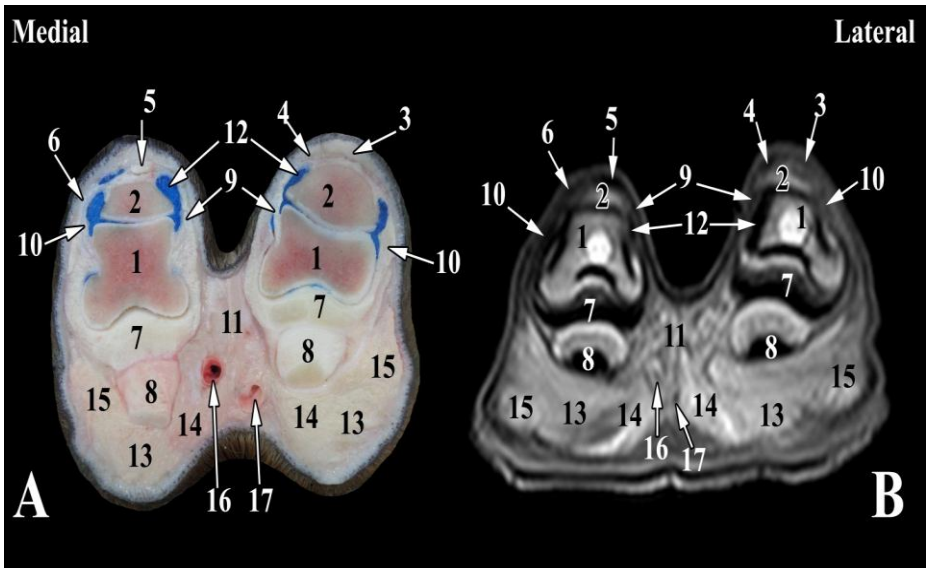

Fig. 4 Transverse images of right hind distal limb of camel at the level of pastern joint. A- Transverse anatomical section; B- Magnetic resonance image:1- Proximal phalanx; 2- Middle phalanx; 3- Lateral digital extensor tendon; 4- Lateral branch of lateral limb of common digital extensor tendon; 5- Medial branch of lateral limb of common digital extensor tendon; 6- Medial limb of common digital extensor tendon; 7- Middle scutum; 8- Deep digital flexor tendon; 9- Axial collateral ligaments of pastern joint; 10- Abaxial collateral ligaments of pastern joint; 11- Interdigital ligament; 12- Joint capsule of pastern joint; 13- Middle digital cushion; 14- Axial digital cushion; 15- Abaixial digital cushion; 16- Proper plantar digital artery; 17- Proper plantar digital vein.

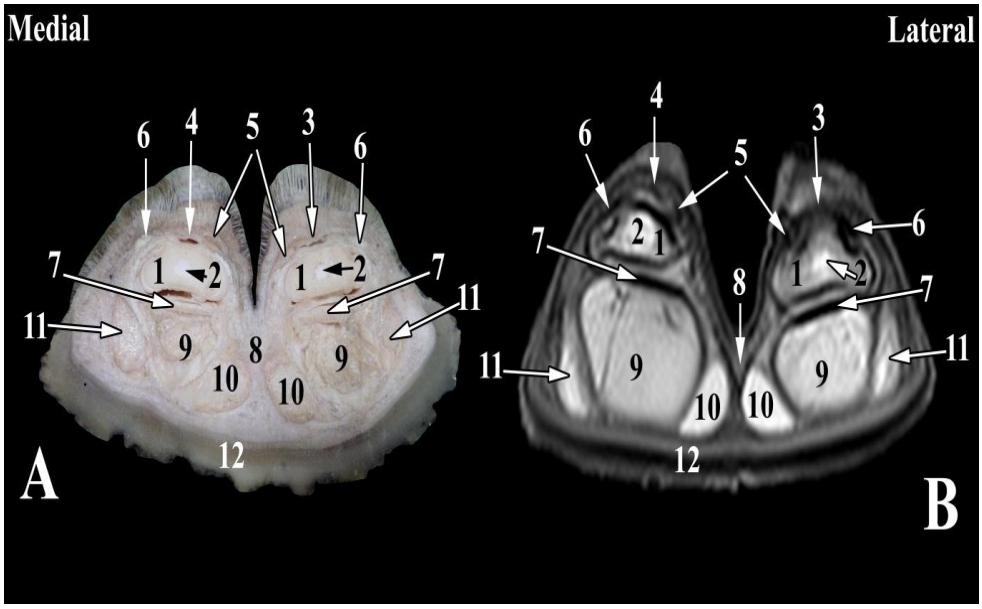

Fig. 5 Transverse images of right hind distal limb of camel at the level of middle of second phalanx (Level 3 as indicated in Fig. 4). A- Transverse anatomical section; B- Magnetic resonance image: 1- Second phalanx; 2- Medullary cavity of second phalanx; 3- Lateral branch of lateral limb of common digital extensor tendon; 4- Medial branch of lateral limb of common digital extensor tendon; 5- Axial dorsal ligaments of coffin joint; 6- Abaxial dorsal ligaments of coffin joint; 7- Deep digital flexor tendon; 8- Interdigital ligament; 9- Middle digital cushion; 10- Axial digital cushion; 11- Abaxial digital cushion; 12- Sole.

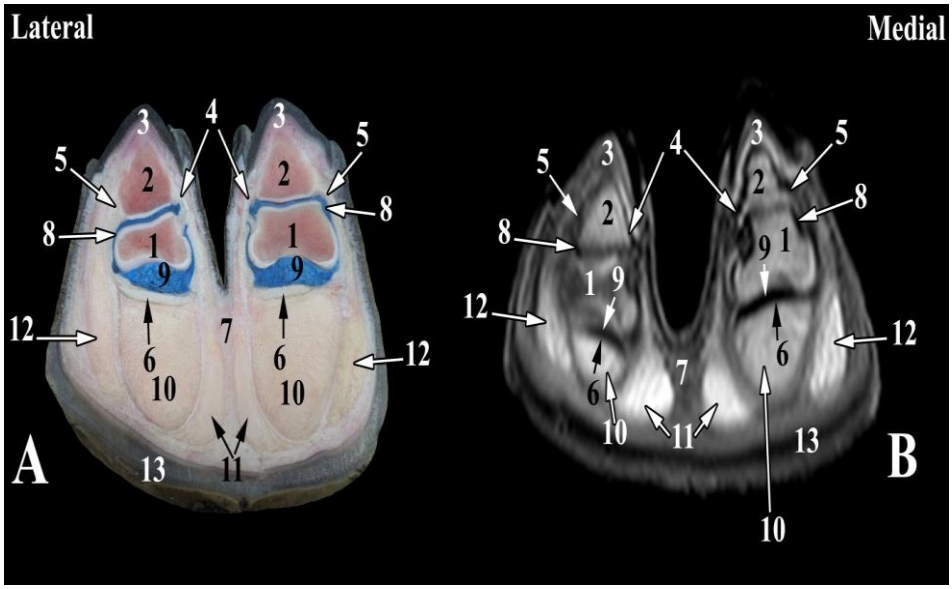

Fig. 6 Transverse images of left hind distal limb of camel at the level of digital cushion. A- Transverse anatomical section; B- Magnetic resonance image: 1- Second phalanx; 2- Third phalanx; 3- Nails; 4- Axial collateral ligaments of coffin joint; 5- Abaxial collateral ligaments of coffin joint; 6- Deep digital flexor tendon; 7- Interdigital ligament; 8- Joint capsule of coffin joint; 9- Plantar synovial pouch of coffin joint; 10- Middle digital cushion; 11- Axial part of digital cushion; 12- Abaxial cushion; 13- Sole.

4. Discussion

MRI was an excellent imaging modality used for scanning of pastern and coffin joints in camel. This modality provided visualization of the most clinically relevant anatomical structures in three planes and serial slices defining these structures at several angles. Also, using latex injected joint capsules allowed a precise characterization of anatomical features of these joints, and provided a standard normal reference for the shape and position of the normal anatomical structures. a T1-weighted MRI was acquired in this study with minimal slice thickness (2mm) and a high acquisition speed allowing more detailed anatomical structures to be appropriate for practical clinical imaging, similarly to the findings of Smith et al. (2011).

Articular cartilages, subchondral bone, cortical bone and cancellous bone were clearly delineated and well-evaluated in the present study. Articular cartilages of second and third phalanges were recognized from the surrounding bony structures as a thin layer of high signal intensity, in matching the findings of Hagag and Tawfiek (2018) in cattle. On contrary, these cartilages could be observed only using CT in horse (Vanderperren et al., 2008). This difficult imaging may be due to markedly curved articular surfaces of the joints and thin cartilages for the spatial resolution during scanning using clinical MRI (Cohen et al., 1999). Moreover, subchondral bone had a low signal intensity and could be clearly differentiated from articular cartilage at extremities of second and third phalanges. Also, cancellous bone could be depicted at extremities of each bone with a high signal intensity, while cortical bone appeared with a low signal intensity (Hagag and Tawfiek, 2018).

The present study reported that medulla of second and third phalanges appeared with high signal intensity on MRI. On the other hand, it appeared with a low signal intensity in cattle (Raji et al., 2009) and camel (El-Shafey and AbdAl-Galil, 2012). Using MRI in this study showed high signal intensity middle scutum and navicular cartilage, heterogeneous high signal intensity digital cushion, and sole appeared as a layer of low signal intensity between two lines of high signal intensity. However, nails of camel and hoof of cattle have a high signal intensity and appear black on MR images (Raji et al., 2009 in cattle; El-Shafey and Abd Al-Galil, 2012 in camel**)**.

The current study provided a detailed visualization of the ligaments of pastern and coffin joints using MRI. These ligaments included; collateral ligaments of pastern joint, as well as the interdigital, collateral and dorsal ligaments of the coffin joint, while palmar/ plantar ligaments of pastern joint and ligaments of navicular cartilage could not be defined. On the other hand, the ligaments of these joints have not been observed in the previous studies (El-Shafey and Abd Al-Galil, 2012; El-Nahas et al., 2015 in camel).

The digital extensor and flexor tendons were evaluated and clearly outlined in cross anatomical sections and their matched MRI. However, these tendons can be evaluated in the cross sections only after removal of the intervening fascia (El-Shafey and Abdel Al-Galil, 2012 in camel). The present study and Hagag and Tawfiek (2018) in cattle visualized these tendons on MR images with low signal intensity. The extensor tendons could be visualized as two oval strips on the dorsum of each digit. In addition, margins of these tendons were well-outlined by the surrounded fascia which had an intermediate signal intensity, similar to the findings of El-Nahas et al. (2015) in camela and Vanderperren et al. (2008) in horse. However, these tendons are visualized as narrow undifferentiated straps on dorsum of each digit on MR images in camel (El-Shafey and Abd Al-Galil, 2012). Moreover, the present study provided visualization of the extensor tendons on MR images as one narrow strip distal to pastern joint which indicated division of lateral limb of the common digital extensor tendon into two branches; each one was ended

in the dorsal ridge of the corresponding third phalanx, on contrary to Smuts and Bezuidenhout (1987) in camel who observed that the extensor tendons don't reach the third phalanges.

The Joint capsules of pastern and coffin joints appeared with low signal intensities, while their margins were clearly delineated as a thin line of intermediate signal intensity on all MR images. Similar results were observed in cattle (Hagag and Tawfiek, 2018). On the other hand, these capsules cannot be observed using MR images, because they are considered as potential cavities and appear only in linear cross sections (El-Shafey and Abd Al-Galil, 2012 in camel).

5. Conclusion

The current study permitted a definite anatomical description of compared cross anatomical sections with their corresponding MR images of the clinically relevant structures of pastern and coffin joints in camel. These images could help as a normal reference during clinical diagnosis of the pastern and coffin joints in camel.

References

Abdellatif AM, Hamed MA, El-Shafaey E, Eldoumani H. (2018). Normal magnetic resonance anatomy of the hind foot of Egyptian buffalo (Bubalus bubalis): A correlative low-field T1- and T2-weighted MRI and sectional anatomy atlas. Anat., Histol., Embryol., 47: 599-608.

Ahmad S, Yaqoop M, Hashmi M, Ahmad S, Zaman MA, Tariq M. (2010). The economic importance of camel: A unique alternative under crisis. Park Vet. J., 30(4):191-197.

Al-Juboori A. (2013). Prevalence and etiology of lameness in racing camels (Camelus dromedarius) in Abu Dhabi Emirate. Journal of Camelid Science, 6: 116–121.

Arencibia A, Vazquez JM, Rivero M, Latorre R, Sandoval JA, Vilar JM, Ramirez JA. (2000). Computed tomography of normal cranio-cephalic structures in two horses. Anat., Histol., Embryol., 29: 295–299.

Cohen ZA, McCarthy DM, Kwak SD, Legrand P, Fogarasi F, Ciaccio EJ, Ateshian GA. (1999). Knee cartilage topography, thickness, and contrast areas from MRI: In-vitro calibration and in vivo measurements. Osteoarthritis and Cartilage, 7: 95-109.

El-Nahas A, Hagag U, Brehm W, Ramadan RO, Al Mubarak A, Gerlach K (2015). Computed tomography of the hind limbs in healthy dromedary camel foot. U. of K. J. Vet. Med. Anim. Prod., 6(2): 98-102.

El-Shafey AA, Abd Al-Galil ASA (2012). Magnetic resonance image of the one-humped (Camelus dromedarius) digits. Journal of American Science, 8(9): 549-556.

Hagag U, Tawfiek MG (2018). Ultrasono-graphy, computed tomography and magnetic resonance imaging of the bovine metacarpo/metatarsophalangeal joint. The veterinary Journal, 233: 66-75.

Monfared AL (2013). Applied anatomy of the head regions of the One-humped camel (Camelus dromedarius) and its clinical implications during regional anesthesia. Global Veterinaria, 10(3): 322-326.

Nuss K, Schnetzler C, Hagen R, Schwarz A, Kircher P (2011). Clinical application of computed tomography in cattle. Tierarztl PraxAusg G Grosstiere Nutztiere, 39(5): 317–324.

Pollard R, Puchalski S (2011). CT contrast media and applications. In: Veterinary computed tomography. Schward, T. and Saunders J. (eds), Willey-Blackwell, pp. 57-65.

Raji AR, Sardari K, Mohammadi HR (2009). Magnetic resonance imaging of the normal bovine digit. Veterinary Research Communications, 33: 515-520.

Sadegh BAM, Shadkhas S, Sharifi A, Mohammadnia HR (2007). Lacrimal apparatus system in one-humped camel of Iran (Camelus dromedarius): Anatomical and radiological study. Iranian Journal of Veterinary Surgery, 2(5):76-80.

Sampson SL, Tucker RL (2007). Magnetic resonance imaging of the proximal metacarpal and metatarsal regions. Clinical Technical Equine Practice, 6: 78-85.

Smith MA, Dyson SJ, Murray RC (2011). The appearance of the equine metacarpo-phalangeal region on high-field vs standing low-field magnetic resonance imaging. Veterinary radiology and Ultrasound, 52: 61-70.

Smuts MMS, Bezuidenhout AJ (1987). Anatomy of the dromedary. Oxford, Clarendon Press, pp. 31-90.

Solano L, Barkema HW, Pajor EA, Mason S, LeBlanc SJ, Zaffino-Heyerhoff JC, Nash CG, Haley DB, Vasseur E, Pellerin D (2015). Prevalence of lameness and associated risk factors in Canadian Holstein-Friesian cows housed in free stall barns. J. Dairy Sci., 98: 6978–6991.

Vanderperren K, Ghaye B, Hoegaerts M, Saunders JH (2008). Evaluation of Computed Tomographic Anatomy of the Equine Metacarpophalangeal Joint. American Journal of Veterinary Research, 69: 631-638.